reported for discrete InGaAsP/InP Franz–Keldysh modulators [4], but it is significantly less than what is obtained from the direct intensity modulation of injection lasers.

In summary, we have demonstrated a monolithically integrated InGaAs/InGaAsP MQW DFB laser with an InGaAs/InAlAs MQW modulator. This integration results in low drive voltage, high switching speed, and low-chirp operation. These results indicate that this device will be useful in high-bit-rate, long-haul optical transmission systems.

ACKNOWLEDGMENT

We thank M. Naganuma and K. Oe for their constructive comments during our discussions, K. Magari for his antireflection coating, K. Sato for his valuable discussions about designing DFB lasers, and H. Tsuchiya and Y. Imamura for their support and encouragement throughout this work.

REFERENCES

[1] Y. Kawamura, K. Wakita, Y. Yoshikuni, Y. Itaya, and H. Asahi, "Monolithic integration of a DFB laser and an MQW optical modulator in 1.5 μm wavelength range," *IEEE J. Quantum Electron.*, vol. QE-23, pp. 915–915, 1987.

[2] M. Suzuki, Y. Noda, H. Tanaka, S. Akiba, Y. Kushiro, and H. Isshiki, "Monolithic integration of InGaAsP/InP distributed feedback laser and electroabsorption modulator by vapor phase epitaxy," *J. Lightwave Technol.*, vol. LT-5, pp. 1277–1285, 1987.

[3] H. Soda, K. Nakai, and H. Ishikawa, "Frequency response of an optical intensity modulator monolithically integrated with a DFB laser," *ECOC'88*, pp. 227–230, 1988.

[4] N. Henmi, S. Fujita, T. Saito, M. Yamaguchi, M. Shikata, and J. Namiki, "A noble dispersion compensation technique for multigigabit transmission with normal optical fiber at 1.5 μm wavelength," *OFC'90*, 1990, paper PD8-1.

[5] T. Kato, T. Sasaki, N. Kida, K. Komatsu, and I. Mito, "Noble MQW DFB laser diode/modulator integrated light source using bandgap energy control epitaxial growth technique," *ECOC'91*, 1991, WeB7-1, pp. 429–432.

[6] M. Aoki, M. Suzuki, M. Takahashi, H. Sano, T. Ido, Y. Kawano, and A. Takai, "High-speed (10Gbit/s) and low-drive-voltage (1V peak to peak) InGaAsP/InGaAsP MQW electroabsorption-modulator integrated DFB laser with semi-insulating buried heterostructure," *Electron. Lett.*, vol. 28, pp. 1157–1158, 1992.

[7] K. Wakita, I. Kotaka, M. Okamoto, H. Asai, Y. Kondo, and M. Naganuma, "High-speed and low-drive-voltage monolithic multiple quantum-well modulator/DFB laser light source," *IEEE Photon. Technol. Lett.*, vol. 4, pp. 16–18, 1992.

[8] T. Kataoka, Y. Miyamoto, K. Hagimoto, K. Wakita, and I. Kotaka, "Ultrahigh-speed driverless MQW intensity modulator and 20 Gb/s, 100 km transmission experiments," *Electron. Lett.*, vol. 28, pp. 897–898, 1992.

8-Element Linear Array Monolithic p-i-n MODFET Photoreceivers Using Molecular Beam Epitaxial Regrowth

Paul R. Berger, Niloy K. Dutta, Dexter A. Humphrey, Peter R. Smith, Shuenn-Jyi Wang,
R. K. Montgomery, D. Sivco, and A. Y. Cho

***Abstract*—An 8-element linear array of single-stage integrating front-end photoreceivers using MBE regrowth was investigated. Each element was comprised of a p-i-n $In_{0.53}Ga_{0.47}As$ photodiode integrated with a selectively regrown pseudomorphic $In_{0.65}Ga_{0.35}As/In_{0.52}Al_{0.48}As$ MODFET. Cutoff frequencies of 1.0 μm discrete regrown MODFET's were $f_t = 24$ GHz and $f_{max} = 50$ GHz. Transconductance of the regrown MODFET's were as high as 495 mS/mm with a current density (I_{ds}) of 250 mA/mm. The 3-dB bandwidth of the photoreceiver was measured to be 1 GHz. The bit rate sensitivity at 1 Gb/s was −31.8 dBm for BER 10^{-9} using 1.55 μm excitation for a photoreceiver with an anti-reflection coating. The single-stage amplifier exhibited up to 25 dB flatband gain of the photocurrent, and a two-stage amplifier was up to 31 dB of gain. Good uniformity between each photoreceiver element in the array was achieved. Electrical crossstalk between photoreceiver elements was estimated to be ~ −34 dB.**

Manuscript received September 4, 1992; revised October 19, 1992.

P. R. Berger was with At & T Bell Laboratories, Murray Hill, NJ 07974. He is now with the University of Delaware, Newark, DE 19716.

N. K. Dutta, D. A. Humphrey, P. R. Smith, S.-J. Wang, R. K. Montgomery, D. Sivco, and A. Y. Cho are with At & T Bell Laboratories, Murray Hill, NJ 07974.

IEEE Log Number 9205953.

INTRODUCTION

OPTOELECTRONIC integrated circuits (OEIC) photoreceivers are nearing the performance level of hybrid photoreceivers when comparing bandwidth and sensitivity. Monolithic photoreceivers have several advantages over hybrid circuits. One advantage of monolithic photoreceivers are reduced size; therefore, reduced parasitics especially due to bond wires which are unnecessary for photodetector and amplifier integration. Another advantage is reduced cost of monolithic circuits; if mass produced, will be cheaper than hybrid circuits. But in all these catagories hybrid circuits will still have some merit. However, when arrays are considered, especially for the stringent design criterion of a wavelength division multiplexed [2] (WDM) lightwave communications system, monolithic photoreceivers are far superior. A WDM system could use an eight color scheme where each discrete wavelength passes for instance 2.5 Gb/s of data. By connecting 8 phototransmitters of slightly different wavelength and launching them into the same optical fiber, a 20 Gb/s system can be realized. At the receiver end, the transmitted signal is separated by passive components into the eight discrete wavelengths and illuminated onto the eight photoreceiver elements. It will be difficult to realize hybrid circuits that will be as compact and as uniform as a monolithic array.

Various schemes for monolithic integration of a photodetector with an amplifier circuit have been employed. The dissimilar epilayers for the photodetector and amplifier can be integrated using three different techniques. The first technique is to grow a single epitaxial growth, one device on top of the other, on an unpatterned substrate [2], [3]. Another approach is a single epitaxial growth on a patterned substrate, and removing the upper device's epilayers with wet chemical etching in particular regions [4]–[6]. The third alternative which we employ is to grow the first epitaxial layer, pattern and etch the wafer, and then regrow the second epitaxial layer into the trench [7]–[10]. This results in a planar wafer with minimal mesa etching needed. We are reporting on an 8-element linear array of single-stage integrating front-end photoreceivers comprised of a p-i-n $In_{0.53}Ga_{0.47}As$ photodiode integrated with a selectively regrown pseudomorphic $In_{0.65}Ga_{0.35}As/In_{0.52}Al_{0.48}As$ 1.0 μm π-gate modulation-doped field effect transistor (MODFET).

EXPERIMENTAL

The p-i-n photodiode is grown by molecular beam epitaxy (MBE) first. The second epilayer is regrown on the same wafer following photolithography and etching of trenches in the first epilayer. Details of the layer structures and processing steps are reported elsewhere [10]. The planar wafer is then processed conventionally to build the OEIC circuit. Isolated p-i-n photodiodes and MODFET's are included in the mask for diagnostic purposes. The MODFET's employ a π-gate configuration to reduce the gate resistance. All gate lengths are 1.0 μm using contact lithography and the gate widths are varied (2×40, 2×75, and 2×100 μm wide). A scanning electron microscope (SEM) photomicrograph of an individual p-i-n MODFET photoreceiver element and three 1×8 OEIC arrays are shown in Fig. 1.

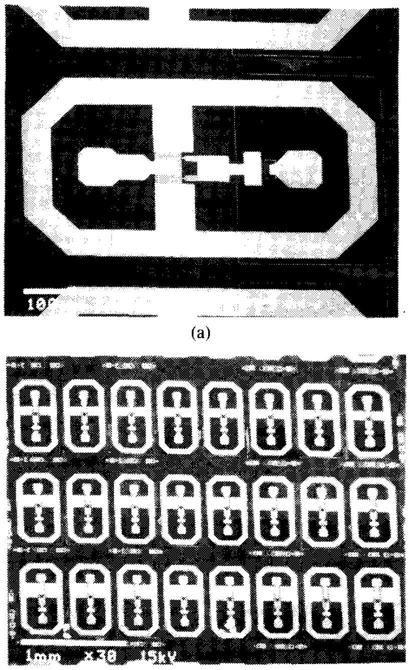

(a)

(b)

Fig. 1. Photomicrograph of (a) the p-i-n MODFET circuit, and three 1×8 arrays.

RESULTS

The dc characteristics of the MODFET's were measured from isolated devices on the same processed wafer as the integrated circuits. The extrinsic transconductance (g_m) of the regrown MODFET's was as high as 495 mS/mm at current densities up to 250 mA/mm at $V_{ds} = 1.5$ V. Compared to as-grown MODFET's, the regrown MODFET's only suffered a roughly 10% dc performance degradation due to regrowth.

Device figures of merit, f_t and f_{max} were measured from 100 MHz to 40 GHz using a vector network analyzer and wide bandwidth coplanar waveguide probes. As-grown MODFET's had cutoff frequencies as high as $f_t = 58$ GHz and $f_{max} = 67$ GHz, while regrown MODFET's ranged up to $f_t = 24$ GHz and $f_{max} = 51$ GHz. The microwave characteristics of 2×40 μm wide as-grown and regrown MODFET's are shown in Fig. 2(a) and (b), respectively. Using the measured S-parameters, equivalent circuits for both MODFET's were obtained. The degraded microwave performance of the regrown MODFET's correlated with the increase in the gate capacitance (C_{gs}) and the slight decrease in the transconductance (g_m). The as-grown MODFET equivalent circuit model resulted in $C_{gs} = 105.7$ fF and $g_m = 46.3$ mS which corresponds to $f_{co} = g_m/(2\pi C_{gs}) = 69.7$ GHz. Similarly, the regrown MODFET model resulted in $C_{gs} = 252.9$ fF and $g_m = 39.5$ mS which corresponds to $f_{co} = 24.8$ GHz.

The dc characteristics were measured of the isolated p-i-n photodiodes which were subjected to regrowth con-

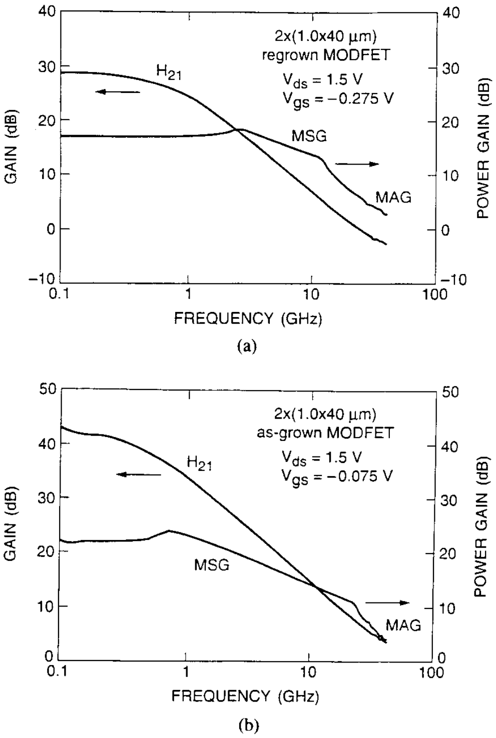

(a)

(b)

Fig. 2. Short circuit current (H_{21}) and power (MSG, MAG) gain of an as-grown 2 × (1.0 × 40 μm) π-gate pseudomorphic $In_{0.65}Ga_{0.35}As/In_{0.52}Al_{0.48}As$ MODFET (V_{ds} = 1.5 V and V_{gs} = −0.075 V). (b) Short circuit current (H_{21}) and power (MSG, MAG) gain of a regrown 2 × (1.0 × 40 μm) π-gate pseudomorphic $In_{0.65}Ga_{0.35}As/In_{0.52}Al_{0.48}As$ MODFFET (V_{ds} = 1.75 V and V_{gs} = −0.275 V).

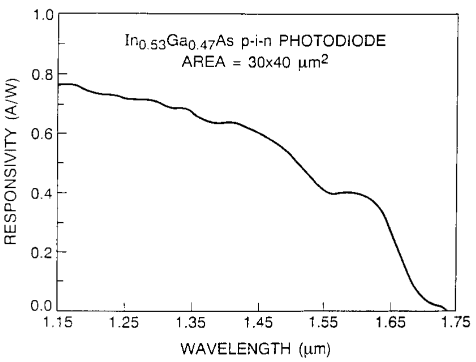

Fig. 3. Spectral responsivity of a 30 × 40 μm^2 p-i-n $In_{0.53}Ga_{0.47}As/In_{0.52}Al_{0.48}As$ photodiode.

ditions, and they exhibited leakage current which ranged from 30 nA to 300 nA at −5 V and breakdown voltages of 18–20 V. The 30 × 40 μm^2 p-i-n photodiode has a junction capacitance of 0.19 pF. The spectral responsivity of the photodiodes was measured using a white light source and a monochrometer. The spectral dependence of the light source was divided out from the responsivity of the photodiode using a commercial photodiode and supplied responsivity curves. The result is shown in Fig. 3. A discrepancy between the actual commercial diode response and the supplied curves accounts for the slight dip in the response around 1.55 μm. The measured responsivity at 1.55 μ is ≥ 0.41 A/W and estimates of the actual responsivity due to the uncompensated large spot size range up to ~0.55–0.60 A/W without antireflection coating (AR).

The bandwidth of the OEIC circuit was measured using a lightwave component analyzer which included a 1.3 μm laser source. The laser output was small signal modulated from 130 MHz–20 GHz. The wafers were probed on-chip with a microwave probe station and laser light was focused onto the photodiode using a fiber-optic probe. The OEIC circuit was biased with V_{ds} = 1.5 V and the photodiode reverse biased at V_p = −4.0 V using bias-T's. The 3-dB bandwidth of the OEIC circuit ranged up to 1 GHz, and was limited by the photodiode bandwidth. No external output buffer or equalizer was utilized. The p-i-n photodiodes were measured in a similar manner and exhibited a 3-dB bandwidth of up to 1.7 GHz. The bandwidth of the photodiodes was limited by a large series resistance created by interaction of the dielectric regrowth mask and the uppermost contact layers during regrowth at elevated temperatures. Similar photodiodes have since been fabricated where a top sacrifical layer is etched off to remove the high series resistance and resulted in photodiode bandwidths in excess of 20 GHz. The flatband gain is calibrated as the response of the OEIC circuit minus the gain of isolated p-i-n photodiodes on the same wafer and measured similarly. The maximum gain of the single-stage OEIC photoreceiver was for a 2 × 100 μm wide gate which exhibited a flatband gain of 24.8 dB. The smallest gate width 2 × 40 μm photoreceiver had a flatband gain of 20.0 dB, and the 2 × 75 μm circuit had a 22.3 dB flatband gain.

The bandwidth of an array of eight p-i-n-MODFET photoreceivers was tested similarly. Fig. 4 shows all eight bandwidth curves for a 2 × 40 μm p-i-n-MODFET photoreceiver array. There is a tight cluster of the eight curves with the bandwidth varying from 509 to 675 MHz. The flatband gain for the eight element OEIC array varied from 20.0 to 17.4 dB. This is very reasonable uniformity, especially for the small test wafer. The roll-off in gain occurred at the edge of the wafer. Arrays with even better uniformity could easily be obtained with this technique using larger, production sized, wafers.

The receiver sensitivity was measured at 1 Gb/s using a 1.55 μm PRBS = $2^{15} - 1$ NRZ signal. The sensitivity as a function of the average power ($\bar{P}$) is plotted and shown in Fig. 5. The receiver sensitivity was measured to be −29.6 dBm for a 2 × 40 μm MODFET at a BER of 10^{-9}. The wafer was then remeasured for sensitivity after deposition of an AR coating. With surface relections minimized, a sensitivity of −31.8 dBm was measured.

Electrical crosstalk between the OEIC photoreceiver elements was estimated using the basic relationship put

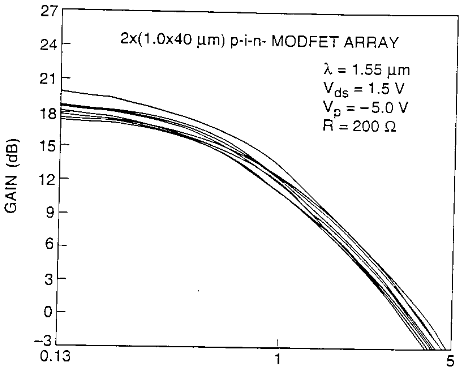

Fig. 4. Measured small signal frequency response of the 8-elements of a monolithic p-i-n-MODFET array using a pseudomorphic 2 × (1.0 × 40 μm) $In_{0.65}Ga_{0.35}As/In_{0.52}Al_{0.48}As$ MODFET (V_{ds} = 1.5 V and V_p = −4.0 V).

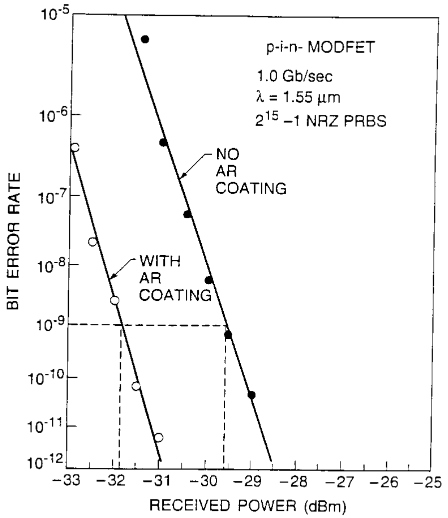

Fig. 5. Sensitivity of the monolithic p-i-n-MODFET circuit using a pseudomorphic 2 × (1.0 × 40 μm) $In_{0.65}Ga_{0.35}As/In_{0.52}Al_{0.48}As$ MODFET (V_{ds} = 1.5 V and V_p = −5.0 V) with and without antireflection (AR) coating.

forth by Kaplan *et al* [11]:

$$|\chi| = \frac{2\pi f R_L C_X}{1 + [2\pi f R_L (C_X + C_T)]^2}$$

where R_L is the load resistance (400 Ω), f is the frequency (1 GHz), C_X is the crosstalk capacitance, and C_T is a parallel combination of the diode capacitance (C_D), the MODFET capacitance (C_{gs}), and all other parasitic capacitances, (C_L). Measurement of C_X was 0.45 nF by probing two adjacent ground rings, and from equivalent circuit modeling C_{gs} = 253 fF dominants C_T. Thus, the electrical crosstalk is estimated to be ~ −34 dB.

The p-i-n-MODFET was also measured as a two-stage amplifier by connecting the drain output of the first p-i-n-MODFET stage to the p-i-n-to-gate connection of a second MODFET. The gate width of the p-i-n-MODFET's measured was 2 × 100 μm. The first p-i-n-MODFET circuit exhibited 19.2 dB of gain, and the second p-i-n-MODFET circuit was 18.9 dB of gain. Combined together, the two-stage photoreceiver demonstrated 30.8 dB of gain with a 3-dB bandwidth of 800 MHz.

SUMMARY

A p-i-n-MODFET photoreceiver was fabricated and tested using MBE selective area regrowth. Cutoff frequencies (f_t and f_{max}) of 58, 67, 24, 51 GHz were measured for the as-grown and regrown MODFET's, respectively. The sensitivity of the p-i-n-MODFET photoreceiver at 1 Gb/s was −31.8 dBm. Excellent element to element OEIC performance uniformity was achieved within the array. Electrical crosstalk of each OEIC element is estimated to be about −34 dB. A two-stage amplifier photoreceiver demonstrated 30.8 dB of gain.

ACKNOWLEDGMENT

We are grateful to Y. K. Chen who provided help with the bandwidth measurements, G. Zydzik who deposited the AR coating, and P. Garbinski for bonding.

REFERENCES

[1] See, for example, Special Issue of Dense Wavelength Division Multiplexing Techniques for High Capacity and Multiple Access Communication Systems, *IEEE J. Select. Areas Commun.*, vol. 8, 1990.

[2] Y. Akahori, M. Ikeda, N. Uchida, A. Kohzen, J. Temmyo, J. Yoshida, T. Kokubun, and K. Suto, "A 622 MB/s monolithically integrated InGaAs-InP high-sensitivity transimpedance photoreceiver and a multichannel receiver array," *IEEE Photon. Technol. Lett.*, vol. 3, pp. 378–380, 1991.

[3] S. Chandrasekhar, L. M. Lunardi, A. H. Gnauck, D. Ritter, R. A. Hamm, M. B. Panish, and G. J. Qua, "A 10 Gbit/s OEIC photoreceiver using InP/InGaAs heterojunction bipolar transistors," *Elect. Lett.*, vol. 28, pp. 466–468, 1992.

[4] W. S. Lee, D. A. H. Spear, P. J. G. Dawe, and S. W. Bland, "Monolithic integration of an InP/InGaAs four-channel transimpedance optical receiver array," *Elect. Lett.*, vol. 26, pp. 1833–1834, 1990.

[5] G.-K. Chang, W. P. Hong, R. Bhat, C. K. Nguyen, H. Shirokmann, L. Wang, J. L. Gimlett, J. Young, C. Lin, and J. R. Hayes, "A novel electronically switched four-channel receiver using InAlAs–InGaAs MSM-HEEMT technology for wavelength-division multiplexing systems," *IEEE Photon. Technol. Lett.*, vol. 3, pp. 475–477 1991.

[6] H. Yano, G. Sasaki, N. Nishiyana, M. Murata, H. Kamiyama, and H. Hayashi, "5 Gbit/s four-channel receiver optoelectronic integrated circuit array for long-wavelength lightwave systems," *Elect. Lett.*, vol. 28, pp. 503–504, 1992.

[7] H. Nobuhara, N. Hamaguchi, T. Fuji, O. Aoki, M. Makiuchi, and O. Wada, "Monolithic pinHEMT receiver for long wavelength optical communications," *Elect. Lett.*, vol. 24, pp. 1246–1248, 1988.

[8] A. Antreasyan, P. A. Garbinski, V. D. Mattera, Jr., H. Temkin, N. A. Olsoon, and J. Flipe, "Monolithically integrated InGaAs-p-i-n InP-MISFET PINFET grown by chloride vapor phase epitaxy," *IEEE Photon. Technol. Lett.*, vol. 1, pp. 123–125, 1989.

[9] Y. Zebda, R. Lai, P. Bhattacharya, D. Pavlidis, P. R. Berger, and T. L. Brock, "Monolithically integrated InP-based front-end photoreceivers," *IEEE Trans. Elect. Dev.*, vol. 38, pp. 1324–1333, 1991.

[10] P. R. Berger, N. K. Dutta, D. A. Humphrey, P. R. Smith, S.-J. Wang, R. K. Montgomery, D. Sivco, and A. Y. Cho, "1.0 GHz monolithic p-i-n MODFET photoreceiver using molecular beam epitaxial regrowth," *IEEE Photon. Technol. Lett.*, vol. 4, p. 891, 1992.

[11] D. R. Kaplan, S. R. Forest, and J. G. Johnson, "Electrical crosstalk in p-i-n arrays," in *Tech. Dig. Conf. Optical Fiber Commun.*, Atlanta, Ga, 1986, p. 100.